POLITECNICO DI TORINO
Repository ISTITUZIONALE

Assessing rockfall risk over time: evolving scenario analysis and management of protective structures

Original
Assessing rockfall risk over time: evolving scenario analysis and management of protective structures / Marchelli, M., Strada, C.. - (2026), pp. 1-8. (XV IAEG World Congress IAEG 2026 Engineering Geology in a Rapidly Changing World Delft (Netherlands) 30/10/2026-06/11/2026) [10.59490/6ad29a514220d0a944d19436].

Availability:
This version is available at: 11583/3017616 since: 2026-11-06T10:36:55Z

Publisher:
IAEG

Published
DOI:10.59490/6ad29a514220d0a944d19436

Terms of use:

This article is made available under terms and conditions as specified in the corresponding bibliographic description in the repository

Publisher copyright

(Article begins on next page)

10 November 2026

https://dx.doi.org/xxxxx/xxxxx

Proceedings of the 15th IAEG World Congress IAEG 2026
Engineering Geology in a Rapidly Changing World
30 October to 6 November 2026
Delft University of Technology, The Netherlands

Assessing rockfall risk over time: evolving scenario analysis and management of protective structures

M. Marchelli[1,*], and C. Strada[2]

[1] Department of Environment, Land and Infrastructure Engineering (DIATI), Politecnico di Torino, C.so Duca degli Abruzzi, 24, 10129, Torino, Italy: Maddalena.marchelli@polito.it, ORCID 0000-0002-9919-2916
[2] Ufficio Geologia e prove materiali, Provincia Autonoma di Bolzano, Via Val d'Ega, 48, 39053 Cardano, Italy; claudia.strada@provincia.bz.it

*corresponding author

ABSTRACT

Quantitative Risk Assessment (QRA) for rockfall hazards is a dynamic and evolving process that must consider not only the current state of the rock slope face and the elements at risk, but also how these conditions may change over time. Traditional single-scenario risk assessments often fail to capture the increasing or shifting nature of risk, potentially leading to under preparedness or inefficient allocation of mitigation resources.

This study presents a time-integrated QRA framework that incorporates a comprehensive range of possible rockfall scenarios. It also proposes strategies to address their evolution, driven by natural processes such as weathering, erosion, and climate change, as well as human-induced factors such as land-use modifications and infrastructure development.

To demonstrate the practical application of this methodology, two case studies at different scales, each requiring varying levels of input data accuracy, are presented. The first case study, at regional scale, applies the framework to the provincial road network of Bolzano, integrating long-term trends in recorded rockfall arrivals, variations in traffic exposure and the time-dependent reliability of mitigation measures into a corridor-scale risk model. The second case study, at slope scale, examines a road section in the Eastern Alps where a windthrow event and subsequent geomorphological disturbances progressively altered block-detachment conditions, reach probabilities and event frequencies, requiring repeated updates to the risk assessment. These examples highlight how integrating the temporal evolution of risk into QRA enhances the accuracy of hazard assessments and supports more strategic, sustainable, and cost-effective risk management.

KEYWORDS: time-integrated risk assessment, risk management, rockfall scenarios, frequency evolution.

INTRODUCTION

Rockfall hazards represent a persistent threat to infrastructure and communities in mountainous regions, where the interplay of geological, climatic, and anthropogenic factors drives complex and evolving risk scenarios. Traditional Quantitative Risk Assessment (QRA) approaches often rely on single-scenario analyses, assuming static conditions for both the rock slope and the exposed elements (Mavrouli et al., 2013; Hantz et al., 2021). While single-scenario approaches may appear adequate for short-term evaluations, they overlook the variability inherent in rockfall processes, particularly the relationship between block volume and event frequency relationship that governs detachment processes and, consequently, the true distribution of hazardous outcomes. Recent studies have highlighted the inadequacy of static models also in the context of climate change, which accelerates slope instability and alters the frequency–magnitude distribution of rockfall events (Farvacque et al., 2019).

A multi-scenario probabilistic framework, as formulated in Marchelli et al. (2025), captures this dynamic nature of risk by integrating a spectrum of possible detachment sizes and their occurrence probabilities. In that formulation, the mean occurrence frequency and the size-dependent detachment probability are combined to define a distribution of possible block volumes. For each admissible volume class, the corresponding energy and height distributions at a given point of interest are described through trajectory-derived intensity functions. The annual risk is then obtained through a double integration over (i) all possible block sizes and (ii) all possible impact intensities (energy or height), within a selected time horizon.

In the present work, the formulation is extended to account for temporal variability, recognising that rockfall hazard and exposure rarely remain static. Progressive changes (e.g., weathering, freeze–thaw cycling, permafrost degradation, glacier retreat) and

Published: dd/mm/yyyy
©2026 published by TU Delft OPEN Publishing on behalf of the authors under CC-BY-4.0 license

instantaneous or one-off modifications (e.g., abrupt slope disturbances, vegetation loss, barrier damage, land-use interventions) can in fact occur. These changes may alter propagation paths and impact probabilities, while evolving traffic patterns or asset relocation modify exposure (Wang et al., 2020). Within the same probabilistic structure, variability is introduced by updating the input functions and parameters that govern the risk calculation. The mean frequency of events may change under environmental forcing; the volume–detachment probability relationship may shift due to modifications in rock-mass structure, weathering state, or the loss of natural energy-dissipation mechanisms; propagation conditions, and thus reach probabilities and impact-intensity distributions, may vary following slope disturbances; vulnerability may evolve with the condition of exposed assets or protective measures; and exposure reflects changes in traffic, operational restrictions, closures, or asset displacement.

When passive protective systems (e.g., net-fence barriers, embankments) are present, residual risk is governed by the protection's failure modes (energy exceedance and height exceedance) and by its time-varying reliability, which depends on inspection outcomes, deterioration, debris accumulation, and maintenance actions (Strada et al., 2015). Embedding reliability updates into the annual recalculation of risk ensures that mitigation effectiveness is quantified consistently over time.

Taken together, these components form a fully probabilistic, time-integrated QRA that weights all plausible scenarios, incorporates both progressive and instantaneous changes, and explicitly tracks the performance of protective measures. This approach supports time-aware risk quantification and enables authorities and asset managers to transition from static, scenario-specific checks to data-driven, adaptive strategies, aligning hazard assessment and mitigation planning with the realities of a rapidly changing mountain environment (Capobianco et al., 2025). In what follows, the mathematical framework for a multi-scenario, fully probabilistic QRA is first provided. Variability in time is then addressed by specifying how changes in environmental, structural, or operational conditions are incorporated into the formulation. Two examples, one at slope scale and one at corridor scale, subsequently illustrate application under differing data requirements and complexity.

METHODOLOGY

Conceptual Framework

Risk on a given element at risk over a time horizon τ is expressed as the expectation of losses arising from all plausible release scenarios, their propagation, impact intensities, vulnerability and exposure. A continuous formulation is adopted, with time-indexed inputs to capture non-stationary behaviour (Marchelli et al., 2025):

$$R(\tau) = E(\tau) W \int_0^\infty \left[1 - e^{-\lambda(\tau) p_d(V_B) p_r^e(V_B)}\right] \left(\int_0^\infty \Psi(v, V_B) f_v(\psi | V_B) dv \right) dV_B \quad (1)$$

where $\lambda(\tau)$ is the mean frequency of block detachment of any size in τ, considering a Poisson point-process, time dependent, $p_d(V_B)$ is the released-volume distribution (conditional on a release), which, together with $\lambda(\tau)$, defines the volume–frequency relationship, $p_r^e(V_B)$ is the reach probability at the element's location, $f_v(\psi | V_B)$ is the distribution of impact velocity (or other intensity measure) conditional on V_B, $\Psi(v, V_B)$ is the vulnerability, or loss ratio, $= E(\tau)$ the exposure, i.e. the probability the element id present when impact occurs, W is the value of the element under the selected loss metric. For each admissible block size, the intensity distribution $f_v(\psi | V_B)$ provides the range of possible energies or impact heights at the considered point. The risk is therefore computed through a double integration, first over all relevant impact intensities and then over all possible volumes.

For rare events, ($\lambda(\tau) p_d p_r^e \ll 1$), the McLaurin expansion yields the usual first-order approximation:

$$R(\tau) \approx E(\tau)\, W \int_0^\infty [\lambda(\tau) p_d(V_B) p_r^e(V_B)] \left(\int_0^\infty \Psi(v, V_B) f_v(\psi | V_B) dv \right) dV_B \quad (2)$$

Where data are sparse, a discrete/binned implementation is convenient: volumes $V_{B,i}$ and intensity bins v_j (e.g., based on percentiles of a velocity distribution) replace the integrals by finite sums, preserving the multi-scenario logic.

If a passive protective system is present upstream, residual risk reflects the failure probabilities of dominant modes (energy exceedance and height exceedance). Let $A_1(V_B)$and $A_2(V_B)$ denote failure probabilities per arrival of a block of size V_B (Marchelli et al., 2021), considering energy and height exceedance, respectively. The residual risk can be written as:

$$R_{res}(\tau) = E(\tau)\, W \int_0^\infty \left[1 - e^{-\lambda(\tau) p_d(V_B) p_r^p(V_B) (A_1(V_B) + A_2(V_B))}\right] \left(\int_0^\infty \Psi(v, V_B) \tilde{f}_v(\psi | V_B) dv \right) dV_B \quad (3)$$

where $p_r^p(V_B)$ is the reach probability at the protection and $\widetilde{f_v}$ accounts for the fact that the protective measure, damaged, might change the reach probability and the velocities of the blocks that eventually arrive at the element at risk. In a very simplified engineering approximation, if the failure probability of the protection system over the time horizon τ is known (e.g., $p_f(\tau) = A_1(\tau) + A_2(\tau)$), and the vulnerability of the element is conservatively assessed under the worst impact scenario (denoted Ψ_{worst}), the risk may be approximated as:

$$R_{res}(\tau) = E(\tau)\, W\Psi_{worst} p_f(\tau) \tag{4}$$

Decision support is obtained by comparing $R(\tau)$and $R_{\text{res}}(\tau)$ against acceptability thresholds, and by evaluating the effectiveness and cost of options: operational exposure management, protective upgrades, additional structures, or asset delocalisation.

Assessing variability of scenarios

The proposed framework explicitly accommodates variability by combining scheduled, time-integrated updates with event-driven revisions whenever conditions change. Rockfall occurrences are therefore treated as a time-dependent (non-stationary) point process whose governing parameters can evolve over time. Treating the process as non-stationary allows all input functions to change, ensuring that risk is recomputed using parameters that reflect both the current state and the expected evolution of the system within the chosen time horizon. By updating these functions whenever new environmental, structural, or operational information becomes available, the framework provides a time-integrated and adaptive quantification of risk, consistent with the dynamic nature of mountain environments.

In particular, progressive drivers of variability, meaning slow, long-term changes such as weathering, freeze–thaw cycles, and permafrost degradation, are handled through regular updates of the mean occurrence frequency $\lambda(\tau)$ and the released-volume distribution $p_d(V_B)$, informed by climate signals (e.g., temperature and precipitation trends, freeze–thaw metrics) and by long-term slope evolution (weathering, changes in roughness, vegetation succession). Trajectory modelling is refreshed to obtain updated reach probabilities $p_r(V_B)$ and impact-intensity distributions $f_v(\psi|\, V_B)$, ensuring that propagation reflects the present configuration of the slope. Asset conditions and the performance of protective measures are incorporated via inspection and maintenance records; the resulting condition classes (e.g., in terms of Defect Level as proposed by UX131 (2025)) translate into revised capacities and failure probabilities $A_1(V_B)$, $A_2(V_B)$ for energy and height exceedance, respectively, or directly $p_f(\tau)$. In this way, gradual environmental and structural changes are captured as drift in hazard, exposure, and mitigation effectiveness.

Superimposed on these slow trends are instantaneous or one-off modifications, i.e. abrupt slope disturbances, vegetation loss, and land-use interventions**,** that may occur sporadically. Following such events, propagation and kinematics are recalculated to reflect altered roughness, deflection and runout paths, directly affecting $p_r(V_B)$ and $f_v(\psi|\, V_B)$. Post-event inspections quantify changes in protective measure capacity, if present, and the residual-risk formulation is immediately updated through $A_1(V_B)$ and $A_2(V_B)$, i.e. $p_f(\tau)$. Operational measures, i.e. temporary closures, detours, or modified traffic schedules, are introduced by adjusting exposure $E(\tau)$; relocation of an element at risk sets exposure to zero for that asset and is reflected at the next re-computation.

Once monitoring, inspection and operational information are consolidated, the risk is recomputed, either in continuous form or via binned approximations, yielding updated values of $R(\tau)$ (without protection) and $R_{\text{res}}(\tau)$(with protection). These are benchmarked against acceptability thresholds and available budgets to support timely decisions: routine or extraordinary maintenance of mitigation measures, addition of complementary protective measures, and exposure management. The full cycle should be documented and scheduled, ensuring that the QRA remains time-aware and adaptive, responsive both to progressive trends and to sporadic events that reshape hazard, exposure, and mitigation reliability.

EXAMPLES OF APPLICATION

Risk assessment on a road network

This example computes the annual risk on a road network exposed to rockfall, adopting the annual probability of at least one victim as the damage metric. The method to compute this social risk centres on arrivals at the road rather than on exhaustive characterisation of detachment at the source (Marchelli et al., 2022). In practice, for road safety management the relevant question is whether a block of any volume above a minimum threshold reaches the road and impacts a vehicle; thus, the hazard can be represented through the arrival rate. Over large extents, full knowledge of the volume–frequency relationship for each source zone is generally unattainable (ontic uncertainties), and the computational burden of trajectory analyses for all sources can be prohibitive. The arrival rate could thus be inferred from continuous recording of events (patrol logs, maintenance reports, sensors). Let $\lambda_r(1y)$ denote the mean number

of blocks that reach the road per year on a given link; the probability of at least one arrival in a year is $1 - e^{-\lambda_r(1y)}$. Within a probabilistic framework coherent with what reported in Eq. (1), the damage, and thus the risk, is assessed through an event-tree approach that considers distinct scenarios potentially leading to a fatality: (i) impact of a block on a vehicle, (ii) impact of a vehicle on a block lying on the carriageway, and (iii) skidding or loss of control due to pavement damage caused by a block. Within this framework, the probabilities that a vehicle is present within the impact footprint at the instant of arrival, or that a vehicle cannot stop in time in the presence of a stationary block or damaged pavement, are computed together with the lethality associated with each scenario. Road geometry and curvature, sight distance, stopping visibility, and the expected traffic (annual flow and speed distributions) are fundamental to obtain the probability of fatality given that at least one block reaches the road, denoted P_{victim} (see Marchelli et al., 2022 for details). The annual risk on a road segment, homogeneous in traffic, geometry, and event recording, is:

$$R(1y) = 1 - e^{-\lambda_r(1y)P_{victim}} \tag{5}$$

The risk is computed per segment, and then summed to obtain the value for the entire network. If mitigation measures are present (e.g., barriers, embankments), their reliability affects the effective arrival rate at the road; in practice, $\lambda_r(1y)$is reduced according to the mitigation system's failure probability $p_f(\tau)$, without changing the event-tree calculation. Accordingly, Eq. (5) becomes:

$$R(1y) = 1 - e^{-\lambda_r(1y)p_f(\tau)P_{victim}}. \tag{6}$$

A baseline calculation at time t_0 proceeds by estimating $\lambda_{\mathrm{r}}^{t_0}(1y)$ on each segment from the recorded number of blocks reaching the road per year, and obtaining $P_{\mathrm{victim}}^{t_0}$and $R^{t_0}(1y)$. The formulation naturally accommodates time variability. If monitoring reveals an increase in arrival frequency (for instance, linked to seasonal climate variability or cryosphere changes), the updated arrival probability becomes $1 - e^{-\lambda_r^{t_1}(1y)}$ and the risk is recomputed accordingly. If operations change (detours, closures, speed reductions), exposure is modified and $P_{\mathrm{victim}}^{t_1}$ is updated before recomputing risk. Finally, where mitigation measures exist, but inspections are overdue, reliability is introduced as an increase of its failure probability.

Considering the road network of the entire Province of Bolzano, the annual individual risk has first been computed under current conditions ("Scenario a"). The baseline hazard is defined through the provincial rockfall event catalogue, which includes systematically recorded events from the last 30 years complemented by historical information. In accordance with the methodology presented earlier, the arrival frequency is not assigned uniformly along a road, but evaluated per portion, reflecting the local variability in source proximity, topography, and historical activity. To ensure spatial consistency across the network, these results are subsequently aggregated into representative 500-m segments, with each segment assigned the maximum annual probability of fatality observed among the portions comprising it (Figure 1a). Exposure is quantified through the average daily traffic (ADT) of each road segment, while the reliability of existing mitigation measures is introduced by classifying each structure into one of five efficiency classes defined through a codified inspection procedure (Gottardi et al., 2011). Each class corresponds to a distinct failure probability and reflects the structure's current condition, including degradation, debris accumulation, and maintenance history. These classes are associated with annual failure probabilities $p_f(1y)$ of 10^{-3}, 0.005, 0.01, 0.1, and 1, ranging from fully efficient to completely ineffective. For network-scale applications, this classification-based approach is justified, as a full reliability analysis for each structure would be impractical. The 500-m sections where no rockfall phenomena occur were excluded from the analysis. Overall, approximately 34% of the 500-m sections of the state and provincial road network managed by the Province of Bolzano are affected by rockfall hazard.

The same formulation has then been applied to three alternative scenarios to reflect plausible variability over time. In "Scenario b", an increase in the arrival frequency is introduced on the basis of recent monitoring trends, which suggest enhanced detachment rates linked to climate-related processes such as more frequent freeze–thaw cycles and the destabilisation of limited permafrost areas, as well as localised increases in hazard associated with vegetation loss caused by *Ips typographus*. Altogether, a 5% increase in arrival frequency is adopted. In "Scenario c", variations in traffic conditions are considered, modifying exposure and occupancy probabilities. Based on observed trends over the last 10 years and projecting them 10 years forward, three classes of increase in ADT are defined: 0% increase for segments with < 1000 vehicles/day, +5% increase for segments with 1000–5000 vehicles/day, +10% increase for segments with > 5000 vehicles/day. In "Scenario d", mitigation measures are assumed to have undergone no maintenance or inspection for five year, in absence of events. A conservative approach is adopted by applying a one-class downgrade in efficiency for each structure, directly increasing the failure probability and thus the effective arrival rate at the road. These four scenarios illustrate how the proposed framework accommodates both progressive and instantaneous changes in hazard, exposure, and protection reliability across an extended linear infrastructure. Table 1 summarises the median, mean, and maximum annual risk values obtained across all 500-m segments for each of the four scenarios. These statistics describe, respectively: (i) the typical level of risk across the network (median), (ii) the tendency of higher-risk values to influence the overall distribution (mean), and (iii) the

most critical situation found anywhere on the network (maximum). As such, the table does not represent individual road sections but the distribution of representative risk values, each derived from maximum-probability portions aggregated over fixed 500-m units. Figure 1 shows the spatial distribution of the annual individual risk across the network under the four scenarios. Compared with the baseline, Scenario b (higher event frequency) produces a coherent but modest increase across all indicators, consistent with a network-wide yet limited intensification of arrivals. Changes in traffic conditions (Scenario c) tend to increase the mean and maximum risk more noticeably, showing that increased ADT magnifies the contribution of segments that are already moderately hazardous, while leaving the typical segment largely unchanged. The scenario reflecting the deterioration of mitigation measures (Scenario d) yields the strongest overall increase, with both the mean and the maximum annual risk significantly exceeding the baseline. This outcome highlights the importance of timely inspection and maintenance: even without changes in hazard or exposure, declines in protection efficiency can materially elevate the network's risk profile.

Table 1. Summary of risk metrics in terms of annual probability of having at least one fatality, $R(1y)$, for the entire Province of Bozen road network across the four scenarios

Scenario	*Description*	*Median annual risk per 500 m on entire network (-)*	*Mean annual risk per 500 m on entire network (%)*	*Maximum annual risk per 500 m on entire network (-)*
a	*Baseline (current conditions)*	1.15×10^{-6}	4.18×10^{-6}	1.39×10^{-4}
b	*Increased event frequency*	1.21×10^{-6}	4.39×10^{-6}	1.46×10^{-4}
c	*Traffic variation (higher exposure)*	1.16×10^{-6}	4.49×10^{-5}	1.53×10^{-4}
d	*No maintenance of mitigation measures*	1.47×10^{-6}	4.93×10^{-6}	1.91×10^{-4}

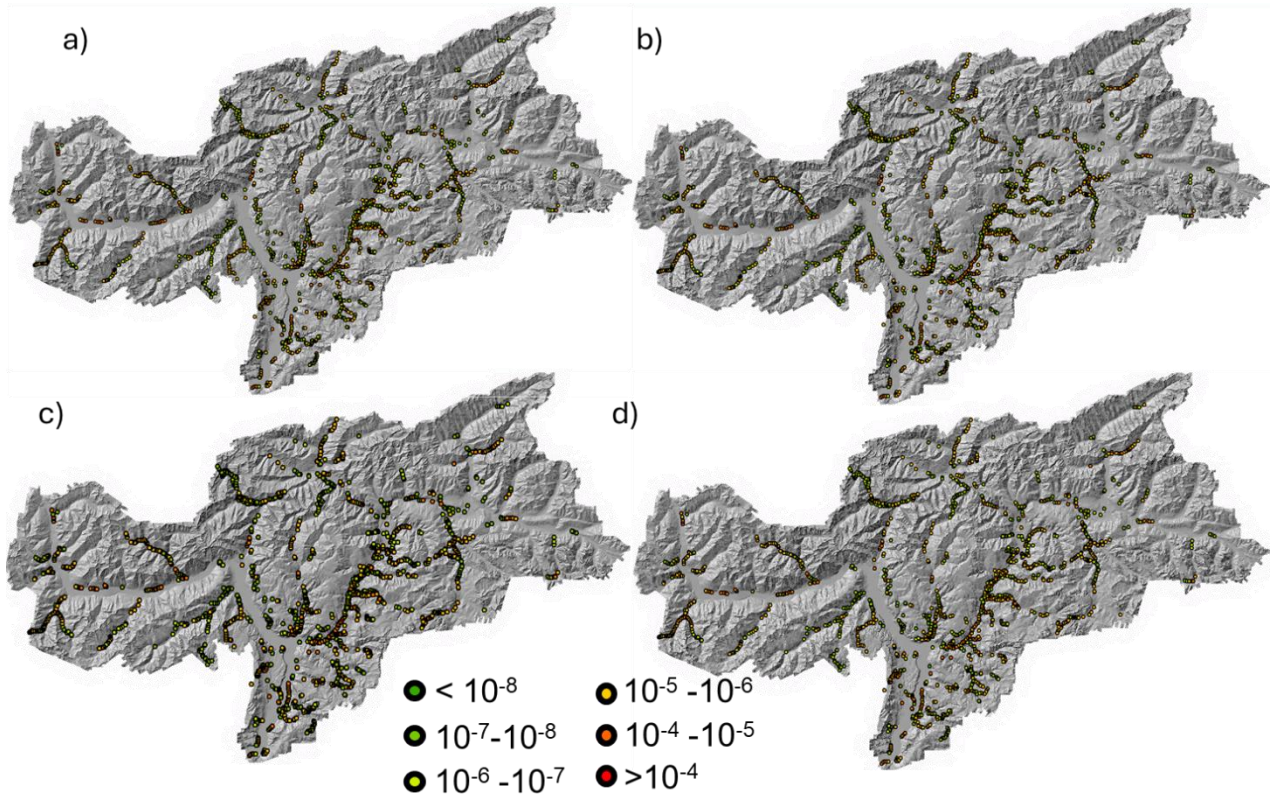


Figure 1 Annual individual risk per 500 m segment for the Province of Bozen road network under the four scenarios (a–d).

Building on this spatial reading of the results and the forward-looking scenarios, the Province has already initiated targeted site inspections and scheduled maintenance and upgrade works on existing protections, prioritising those 500-m units that display the most marked increases in the indicators, so as to translate the analysis into prompt, tangible risk-reduction actions.

Risk assessment on a single slope

The second example illustrates the framework at slope scale, where detailed input data and site-specific conditions permit a more refined analysis. As in the network-scale case, the social risk on a road is assessed, but here the reduced extent allows explicit consideration of source zones, volume–size distributions, and trajectory simulations for different block sizes.

Along the SS 620 between km 2.40 and km 2.75 on the Lavazè Pass (Province of Bozen, Italy), the road runs along a slope where rockfall activity has been observed occasionally (Figure 2). On 6 July 2019, a widespread windthrow event occurred in the Eggental valley, severely affecting the steep slope above this section of the SS 620. Almost all conifers were knocked down over an area of approximately 3 ha, and the existing passive rockfall protection structures were completely destroyed. Several blocks reached the carriageway, and further unstable boulders were identified during subsequent inspections. Clean-up operations and removal of damaged timber were initiated immediately. The uprooting of trees and subsequent timber removal exposed large areas of bare soil, creating additional susceptibility to surface erosion. On 3 November 2019, intense rainfall triggered a landslide of approximately 20 m³ over an area of about 50 m², significantly altering the slope morphology. Additional individual blocks also reached the road.

Prior to the July 2019 event, the slope exhibited only limited instability: sporadic detachments of small blocks (0.1–0.5 m³) were occasionally observed within the Atesina volcanic rocks of the Ora Formation. The loss of forest cover created extensive surface "wounds", drastically reducing the protective function of vegetation and increasing exposure to meteorological forcing. As a result, the volume of potentially detachable blocks increased to 1.2–2 m³. Detailed trajectory analyses indicated a maximum reach probability to the road of 5–10% and maximum expected impact energies of approximately 1,500–2,000 kJ. Applying the method proposed earlier in the paper and Eq. (5), and considering an ADT of approximately 800 vehicles/day, the annual social risk, in absence of mitigation measures, was $4.68 \cdot 10^{-5}$.

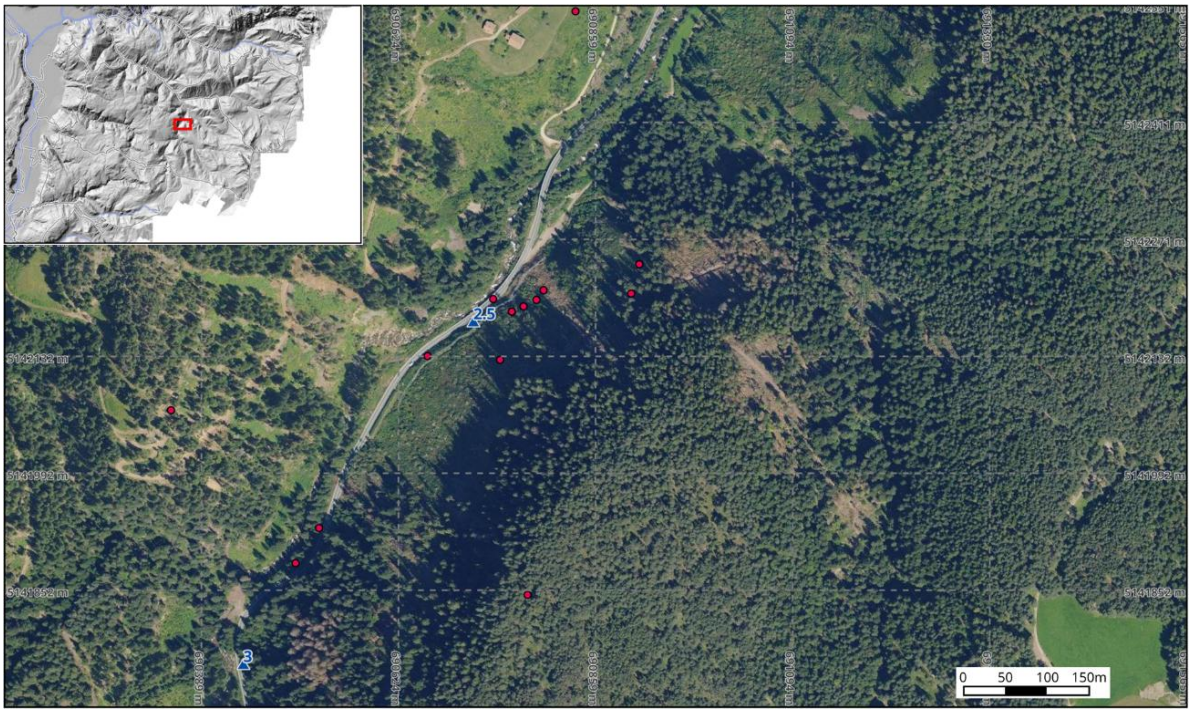


Figure 2 Overview of the SS 620 road section between km 2.40 and km 2.75 on the Lavazè Pass (Province of Bozen, Italy) (source: https://mapview.civis.bz.it/). Past rockfall events are shown as red dots, whereas blue triangles indicate the kilometre markers along the carriageway.

In the following years, the widespread disturbance of the soil and vegetation initiated a retrogressive destabilisation process. Pre-existing fractures in the upper outcrops progressively widened, favouring the detachment of larger blocks up to 4–5 m³, with a high likelihood of reaching the road due to the absence of the forest that had previously dissipated energy. As an example, on 26

April 2023, a rockfall occurred at km 2+400 on the SS 620: a rootstock above the road toppled, triggering two porphyry blocks, the larger of which had a volume of approximately 1 m³. Using the updated DTM reflecting the post-event configuration, recalculated trajectories indicate a maximum reach probability approximately eight times higher than pre-event conditions. Under these new conditions, and in the absence of functional mitigation measures, the annual social risk in absence of mitigation measures increases to $2.81 \cdot 10^{-4}$, reflecting the combined effect of (i) the higher frequency of detachment and (ii) the significantly increased reach probability. The now possible larger block volumes and higher impact energies should be considered to ensure that any mitigation measures adopted are sufficiently effective. Specifically, in a location suitable for installing a rockfall barrier, a 5000 kJ, 6 m-high system is now required to reduce the annual social risk to $2.81 \cdot 10^{-7}$.

This example clearly illustrates how a sudden disturbance, such as a localised windthrow, can drastically modify both the hazard and the risk profile within a very short timescale, highlighting the necessity of time-integrated and updateable QRA approaches.

CONCLUSION

This work introduces a time-integrated, multi-scenario probabilistic framework for rockfall risk assessment that accounts for the full volume–frequency relationship and the distribution of impact intensities. By allowing input functions to evolve, the method captures both progressive changes (e.g., weathering, freeze–thaw, permafrost degradation) and sudden, event-driven modifications such as slope disturbances or degradation of protective systems. Residual risk is consistently evaluated through reliability-based failure modes.

Applications at corridor and slope scale demonstrate that rockfall risk is highly sensitive to variations in event frequency, exposure, and mitigation performance, and that single-scenario, static approaches may underestimate critical changes. The framework supports adaptive and cost-effective management, offering a practical basis for updating risk evaluations and prioritising interventions in dynamic mountain environments.

ACKNOWLEDGEMENTS

This work was supported by Marie Curie Postdoctoral Fellowship 2022 (Call Horizon-MSCA-2022-PF-01, grant GA101103401 - RIDETHERISK project) and by the Roads Service and the Geological Service of the Autonomous Province of Bolzano

CONTRIBUTION STATEMENT

Conceptualization: MM & CS; Data Curation: MM & CS; Analysis: MM & CS; Methodology: MM; Visualization: MM & CS; Writing: MM; Funding acquisition: MM; Project administration: MM & CS; Validation: MM & CS.

REFERENCES

Capobianco, V., Choi, C. E., Crosta, G., Hutchinson, D. J., Jaboyedoff, M., Lacasse, S., ... & Reeves, H. (2025). Effective landslide risk management in era of climate change, demographic change, and evolving societal priorities. Landslides, 1-19. https://doi.org/10.1007/s10346-024-02418-2

Farvacque, M., Lopez-Saez, J., Corona, C., Toe, D., Bourrier, F., & Eckert, N. (2019). How is rockfall risk impacted by land-use and land-cover changes? Insights from the French Alps. Global and Planetary Change, 174, 138-152. https://doi.org/10.1016/j.gloplacha.2019.01.009

Gottardi, G., Govoni, L., Mentani, A., Ranalli, M., & Strada, C. (2011, June). The effectiveness of protection systems toward rockfall risk mitigation. In *Proc. 3rd int symp on geotech safety and risk. By edited Straub and Bräu* (pp. 157-164).

Hantz, D., Corominas, J., Crosta, G. B., & Jaboyedoff, M. (2021). Definitions and concepts for quantitative rockfall hazard and risk analysis. *Geosciences*, *11*(4), 158. https://doi.org/10.3390/geosciences11040158

Marchelli, M., De Biagi, V., & Peila, D. (2021). Reliability-based design of rockfall passive systems height. International Journal of Rock Mechanics and Mining Sciences, 139, 104664. https://doi.org/10.1016/j.ijrmms.2021.104664

Marchelli, M., De Biagi, V., Bertolo, D., Paganone, M., & Peila, D. (2022). A mixed quantitative approach to evaluate rockfall risk and the maximum allowable traffic on road infrastructure. Georisk: Assessment and Management of Risk for Engineered Systems and Geohazards, 16(3), 584-594. https://doi.org/10.1080/17499518.2021.2010097

Marchelli, M., De Biagi, V., & Chiaia, B. (2025). A fully probabilistic framework to compute the residual rockfall risk in presence of mitigation measures. Landslides, 22(9), 2961-2968. https://doi.org/10.1007/s10346-024-02377-8.

Mavrouli, O. C., Abbruzzese, J., Corominas, J., & Labiouse, V. (2013). Review and advances in methodologies for rockfall hazard and risk assessment. In *Mountain risks: From prediction to management and governance* (pp. 179-199). Dordrecht: Springer Netherlands. https://doi.org/10.1007/978-94-007-6769-0_6

Strada, C., Tagnin, S., Mottironi, M., Larcher, V., Villa, G., & Mair, V. (2015). Management of Rock Fall Risk on the Main Roads of Southtirol. In Engineering Geology for Society and Territory-Volume 2: Landslide Processes (pp. 1829-1833). Cham: Springer International Publishing. https://doi.org/10.1007/978-3-319-09057-3_324

UX131 – Metodologia per la gestione delle barriere paramassi a rete esistenti attraverso l'individuazione di classi di attenzione in funzione del rischio (2025), UNICMI, Unione Nazionale delle Industrie delle Costruzioni Metalliche dell'Involucro e dei serramenti

Wang, X., Frattini, P., Stead, D., Sun, J., Liu, H., Valagussa, A., & Li, L. (2020). Dynamic rockfall risk analysis. *Engineering Geology*, *272*, Article 105622. https://doi.org/10.1016/j.enggeo.2020.105622